International Journal of Energy Science (IJES) Volume 4 Issue 3, June 2014 www.ijesci.org
doi: 10.14355/ijes.2014.0403.05

Production of 14 MeV Neutrons Using Pyroelectric Crystals: Reconverting Solar Energy into Nuclear Fusion Energy

Werner Tornow

Department of Physics, Duke University and Triangle Universities Nuclear Laboratory, Durham, NC, USA
tornow@tunl.duke.edu

Received 19 March 2014; Accepted 27 March 2014; Published 25 April 2014

Abstract

By changing the temperature of a $LiTaO_3$ pyroelectric double-crystal arrangement in a deuterium gas environment, deuterium ions were produced and accelerated towards a tritiated target, producing 14 MeV neutrons via the $^3H(d,n)^4He$ nuclear fusion reaction.

Keywords

Nuclear Fusion; Fusion Reactions in the Sun; Neutron Production; Pyroelectric Crystals

Introduction

In continuation of our previous work which has focused on initiating the $^2H(d,n)^3He$ nuclear fusion reaction with a pyroelectric double-crystal arrangement (Tornow et al, 2010), we turned our attention to the $^3H(d,n)^4He$ nuclear fusion reaction with the goal of producing 14 MeV neutrons. At a first glance this task seems easier than that involving the $^2H(d,n)^3He$ reaction with its relatively small Q-value of +3.27 MeV and its very small reaction cross section of about 16 mb at 100 keV, compared to +17.59 MeV and almost 5000 mb, respectively, for the $^3H(d,n)^4He$ reaction. However, the safety requirements associated with the use of tritium, and another tritium-target related issue, pose severe constraints on operating our standard pyroelectric crystal apparatus in a university environment.

Although the $^3H(d,n)^4He$ reaction is not very important to our Sun's energy production, it does take place in the Sun, and it is generally considered as the most practical candidate to reach or even exceed the break-even point in a controlled fashion on Earth, for example, at the National Ignition Facility (NIF)[1] at Lawrence Livermore National Laboratory, or at the International Thermonuclear Experimental Reactor (ITER)[2] at Cadarache in France.

A number of conflicting publications exist about the yield of neutrons produced in another fusion reaction, the $^2H(d,n)^3He$ reaction. The work of the RPI group (Geuther, Danon, and Saglime, 2006; Geuther and Danon, 2007; Gillich et al, 2009) provides convincing evidence that neutrons were produced via this reaction. However, doubts exist that the earlier work of the UCLA group (Naranjo, Gimzewski, and Putterman, 2005; Tang et al, 2007) has ever produced the reported number of $^2H(d,n)^3He$ neutrons. As has been shown in (Tornow, Shafroth, and Brownridge, 2008), any pulse-height signals due to 2.5 MeV neutrons obtained with not sufficiently shielded neutron detectors are buried under pile-up events originating from the intense X-ray radiation present in pyroelectric crystal experiments. The suspicion appears to be confirmed by the UCLA group's recent work involving the $^3H(d,n)^4He$ reaction (Naranjo, Putterman, and Venhaus, 2011). In Figure 5 of (Naranjo, Putterman, and Venhaus, 2011) the pulse-height region identified to be associated with $^3H(d,n)^4He$ neutrons appears to be again due to pile-up X-ray events, which are misidentified as neutrons in the pulse-shape discrimination electronics (Tornow, Shafroth, and Brownridge, 2008). This conclusion seems also to be supported by their yield versus deuteron energy curve (Figure 3 in (Naranjo, Putterman, and Venhaus, 2011)) which does not follow

[1] See https://lasers.llnl.gov
[2] See https://www.iter.org/proj

the energy dependence of the $^{3}H(d,n)^{4}He$ cross section and the range of the ions in the tritiated target. It is not known whether or not the UCLA group has checked on their results by replacing the deuterium gas by regular hydrogen gas, as was done in Refs. (Tornow et al, 2010; Tornow, Shafroth, and Brownridge, 2008). In this case, neutrons cannot be produced.

Experimental Arrangement

A schematic view of our experimental setup is shown in Figure 1. It consists of a cylindrical chamber made of aluminum, which houses the pyroelectric two-crystal arrangement. The 1 inch diameter and 1 inch long $LiTaO_3$ crystals and their heating/cooling modules were glued onto a copper frame with good heat contact to the chamber. The thermoelectric modules (based on the Peltier effect) were of the type Melcor HT6 obtained from Laird Technologies[3]. The maximum current and voltage used in our work were 3 A and 4 V, respectively, values which can be provided by a small solar panel. The distance between the crystals was 4.3 cm. The crystals were purchased from Red Optronics[4], as were all the crystals employed in our previous works (Tornow et al, 2010; Tornow, Shafroth, and Brownridge, 2008; Tornow, Lynam, and Shafroth, 2010). However, the new crystals, when tested individually, never provided acceleration potentials in excess of 130 kV, although they were conditioned using our standard approach involving up to 40 heating and cooling cycles between room temperature, 130° C, and 0° C. Typically, discharges occurred already at 120 kV, in contrast to our previous work (Tornow, Lynam, and Shafroth, 2010), where acceleration potentials between 250 and 300 kV were achieved quite routinely. The reason for the inferior performance of the new crystals is unknown. Unfortunately, the pyroelectric crystals used in (Tornow et al, 2010; Tornow, Shafroth, and Brownridge, 2008; Tornow, Lynam, and Shafroth, 2010) have developed cracks caused by too rapid temperature changes, and therefore are not useful anymore.

As can be seen in Figure 1, a tritiated-titanium target was attached to the z+ face of the left crystal, facing the z- face of the other crystal. The tritiated-titanium target was obtained from SODERN[5], and consisted of a 19 mm diameter and 0.4 mm thick disk of copper with a titanium layer evaporated onto it. The thickness of the titanium layer was 2.1 mg/cm^2 with a diameter of 16 mm. It was loaded with 1.9 Ci of tritium. A teflon ring kept the tritiated-titanium target in place.

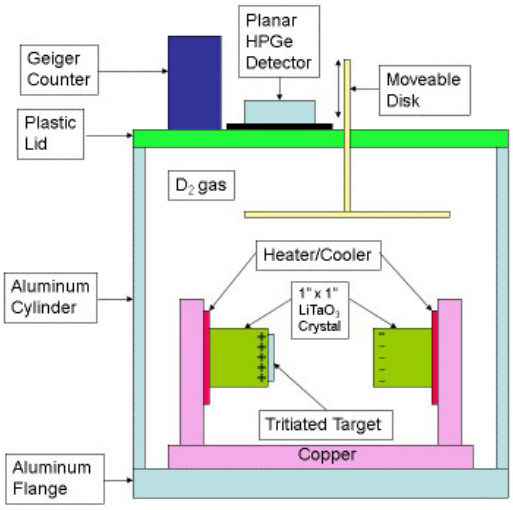

FIGURE 1 SCHEMATIC OF DOUBLE-CRYSTAL ARRANGEMENT WITH TRITIATED TARGET ATTACHED TO THE $LiTaO_3$ CRYSTAL TO THE LEFT, AND GEIGER COUNTER AND HIGH-PURITY GERMANIUM (HPGE) DETECTOR PLACED ON TOP OF THE CHAMBER

Two 5 inch diameter and 2 inch thick BC-501A neutron detectors[6], each enclosed by a 1.25 cm thick lead housing, were positioned outside of the chamber at backward angles relative to the direction from the naked $LiTaO_3$ surface towards the crystal with the tritiated-titanium target attached to (see Figure 2). The center-to-center distance between each neutron detector and the tritiated target was 12.5 cm. The neutron detectors had neutron-gamma pulse-shape discrimination (PSD) properties and were connected to an MPD-4 module[7], which provided amplified pulse-height signals and pulse-shape signals with clear separation between gamma-ray/X-ray and neutron induced events (see Figure 6 of Ref. (Tornow et al, 2010)). A planar High-Purity Germanium (HPGe) detector[8] was placed above the chamber to monitor the X-ray radiation produced, and to determine its maximum energy, which is a measure of the acceleration potential between the two crystals. The entire apparatus was operated in a target room at TUNL, which provided the necessary infrastructure to vent fore-pump exhaust gases from chambers or beam lines containing tritiated targets.

[3] Laird Technologies (http://www.lairdtech.thomasnet.com)
[4] See http://www.redoptronics.com for pyroelectic crystals
[5] EADS Sodern North America Inc. (www.sodernusa.com)
[6] Bicron 501A liquid scintillator supplied by Saint Gobain Crystals (www.detectors.saint-gobain.com)
[7] MPD-4 Pulse-Shape Discrimination module supplied by Mesytec (www.mesytec.com)
[8] ORTEC Model GLP-36385/13S (www.ortec-online.com)

Measurement Procedures

In our previous work (Tornow et al, 2010) involving the $^{2}H(d,n)^{3}He$ reaction, the $LiTaO_3$ crystals including their deuterated polyethylene coated front faces were heated up to 130° C and subsequently cooled to about 0° C in a deuterium gas environment of a few mTorr. Although tritiated-titanium targets are known to not release any substantial amounts of tritium at temperatures below 200° C (Marion and Fowler, 1960), the maximum temperature was limited in the present study to 80° C to provide a comfortable safety margin. Because the electric potential achievable with pyroelectric crystals depends on the temperature change ΔT, this restriction resulted in a considerable loss of acceleration potential.

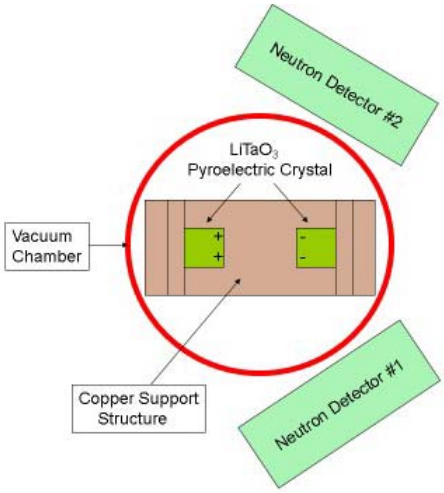

FIGURE 2 SCHEMATIC OF TOP VIEW OF CHAMBER SHOWN IN FIGURE 1, INDICATING THE LOCATION OF THE TWO NEUTRON DETECTORS

Heating Cycle

A typical heating cycle consisted of heating the crystals from room temperature up to 80° C in 800 seconds in vacuum of better than 10^{-4} Torr. Due to the developing polarization charge and the associated strong electric field, free electrons are produced in the vicinity of the crystal faces and accelerated towards the z+ crystal carrying the tritiated-titanium target, while the resulting positively charged residual-gas ions are accelerated toward the z^- crystal. The potential difference between the two crystal surfaces was monitored by recording the X-ray energy spectrum produced when accelerated electrons were hitting the tritiated-titanium target, its copper backing, and the crystal itself. The potential never exceeded 100 kV. To reduce the count rate in the HPGe detector to a manageable level, the X-ray flux was attenuated by a 3 mm thick lead absorber. The radiation recorded with a Geiger counter placed on top of the chamber also gave a good indication of the acceleration potential. In our setup the current between the two crystals could not be measured directly. Instead, an insulated aluminum disk was mounted just above the two crystals to collect the "stray current" which turned out to be proportional to the rate in the HPGe detector and the radiation level obtained with the Geiger counter. Typical maximum current and radiation readings were +0.05 nA and 5 mrem/h, respectively. We normally kept the crystals at their maximum temperature for up to 90 minutes. During this time interval we experienced typically two to three discharges, resulting in close to zero potential and current. After each discharge, the potential and current increased again, indicating that the bottom and top face of each crystal were not in thermal equilibrium yet. Finally, after the current dropped and stayed below 0.002 nA, the valve to a deuterium gas bottle was opened and the chamber was pressurized to the desired deuterium pressure, typically 10 mTorr.

Cooling Cycle

After waiting for about 5 minutes the crystals were cooled to 0° C in 600 seconds. Now the developing polarization charges are reversed compared to the heating case, i.e., positively charged deuterium ions are created and accelerated toward the crystal with the tritiated target attached to. If the energy and the current of the deuterium ions are large enough, neutrons will be produced via the $^{3}H(d,n)^{4}He$ reaction. From the HPGe detector spectra we concluded that on the average maximum acceleration potentials of about 150 kV were achieved in the present work. This corresponds to 75 kV for an individual crystal, which is in line with the reduced ΔT, compared to the 130 kV referred to earlier by cooling from 130° C to 0° C. During the cool-down process we typically experienced three to five discharges. However, after the third discharge the potential typically did not reach values anymore which were useful for neutron production. Maximum currents and radiation readings of -0.2 nA and 20 mrem/h, respectively, were obtained during the cool-down phase.

The neutron production cross section has a very pronounced maximum at the deuteron energy of about 106 keV. The deuterium ions produced in our work consist of D_2^+ ions, as was shown in (Tornow, Taylor, and Shafroth, 2011) by employing a magnetic-field deflection technique. Therefore, with a maximum acceleration potential of 150 kV, the maximum energy available for neutron production is only 75 keV.

Furthermore, a dead layer developed on the tritiated-titanium target surface already during the first heating/cooling cycle, which turned the color on its surface from originally gray to dark black after a few heating/cooling cycles. This oxidation effect has been observed also by the RPI group when they tried to use deuterated-titanium targets for producing $^{2}H(d,n)^{3}He$ neutrons (Danon, 2011). The UCLA group (Naranjo, Putterman, and Venhaus, 2011) refers to a developing dead layer on their tritiated target as well. In our case, this dead layer of unknown thickness reduced the available D_2+ ion energy even further. We estimate that our effective maximum deuteron energy is about a factor of two lower than the 106 keV needed to be on top of the $^{3}H(d,n)^{4}He$ resonance. In addition, the range of 50 keV D_2+ ions in titanium is only about 1/10 of the titanium layer thickness of 5 µm. Therefore, the effective tritiated target thickness is extremely small.

Results

Even with such a low maximum effective deuteron energy and thin target thickness, neutrons were produced via the $^{3}H(d,n)^{4}He$ reaction in the present work. Figure 3 shows a plot of (a) pressure, (b) temperature, (c) current, (d) X-ray radiation, (e) maximum X-ray energy, and (f) number of recorded neutrons in neutron detector #1 versus time, obtained during the cool-down phase from 80° C to 0° C in one of the early runs. As can be seen, three discharges occurred during this time period, and 26, 12 and 2 neutrons above background were produced before the 1nd, 2rd, and 3rd discharge, respectively. The natural neutron background rate in this detector was 0.9 neutrons per minute in the energy region of interest. Just before the 1st discharge the current reached its maximum value and the maximum X-ray energy was 150 keV, resulting in a total of 26 neutrons above background. After this discharge, the current and potential, as measured by the X-ray energy, increased again, but both quantities did not reach the values recorded just before the 1st discharge. Therefore, it is not surprising that only 12 neutrons were observed during this time period. Finally, the 3rd discharge occurred at very low current and a maximum potential of only 100 keV was achieved, resulting in 2 neutrons only. Figure 4 is similar to Figure 3, but it is based on one of our later runs. Here, four discharges occurred. Just before the 4th discharge, the maximum X-ray energy reached 182 keV, but the current was lower than before the 3rd discharge. The recorded neutron yield in det #1 above background before the 1st, 2nd, 3rd and 4th discharge was 4, 0, 17, and 17, respectively.

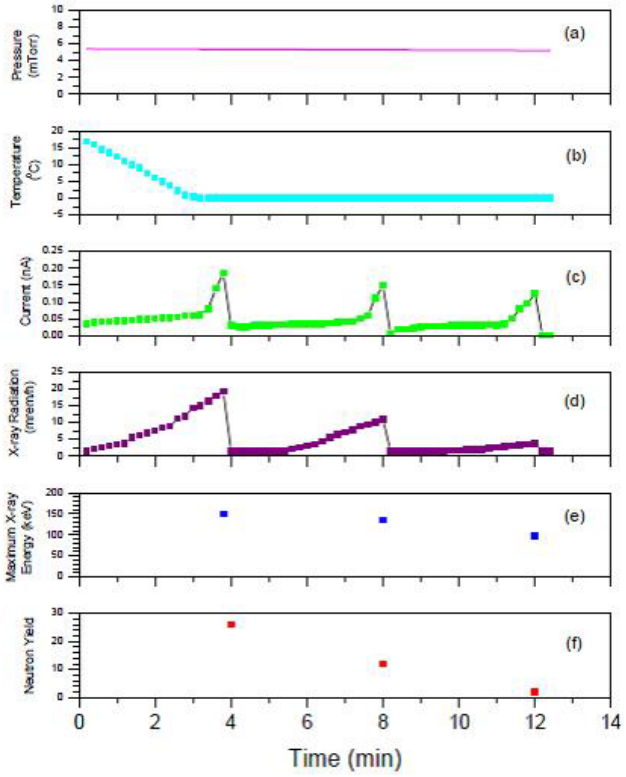

FIGURE 3 PARAMETERS MONITORED DURING COOL-DOWN PHASE OF PYROELECTRIC CRYSTALS AS FUNCTION OF TIME FOR A RUN IN THE EARLY STAGE OF OUR MEASUREMENTS: (a) PRESSURE, (b) TEMPERATURE, (c) CURRENT MEASURED ON THE DISK SHOWN IN FIGURE 1, (d) RADIATION LEVEL MEASURED WITH GEIGER COUNTER SHOWN IN FIGURE 1, (e) MAXIMUM X-RAY ENERGY RECORDED WITH HPGe DETECTOR SHOWN IN FIGURE 1, AND (f) NEUTRON YIELD ABOVE BACKGROUND OBTAINED BETWEEN DISCHARGES (SEE TEXT)

Figure 5 represents a two-dimensional spectrum of pulse height (y axis) versus pulse-shape parameter (x axis) of neutron detector #1, which had an energy threshold of 1 x ^{137}Cs, the pulse height of the Compton edge produced by 662 keV gamma rays in the liquid scintillator BC 501A. This pulse height corresponds to a neutron energy of about 2 MeV (Gonzalez Trotter et al, 2009). The intense band of events with pulse-shape parameter values of about 1185 or smaller are produced by X-ray pile-up events and gamma rays from the environment, including cosmic-ray induced gamma rays, while the much less intense band of events to the right is caused by neutrons from the reaction of interest and from cosmic-ray neutrons. The spectrum shown in Figure 5 is the sum of 9 cool-down phases totaling 19 individual time periods during which neutrons were produced. The total neutron production time was 74.3 minutes, resulting in 2.8 neutrons per minute. A two-dimensional gate was set on the neutron bands and projected across onto the y-

axis, to produce the neutron energy spectrum shown by the solid-line histogram in Figure 6 (a). The same was done for a 74.3 minute background spectrum obtained without cooling the pyroelectric crystal arrangement. This spectrum is shown as the dashed-line histogram in Figure 6 (a), indicating an excess of neutron events with a foreground to background ratio of 3.25. Finally, Figure 6 (b) represents the difference spectrum. This spectrum contains 144 neutron events, resulting in a neutron production rate of 1.94 neutrons per minute. The measured counts exceed the background by 5.3 standard deviations. The results obtained with neutron detector #2 were similar to those obtained with neutron detector #1. In the former case, we recorded a total of 106 neutrons above background.

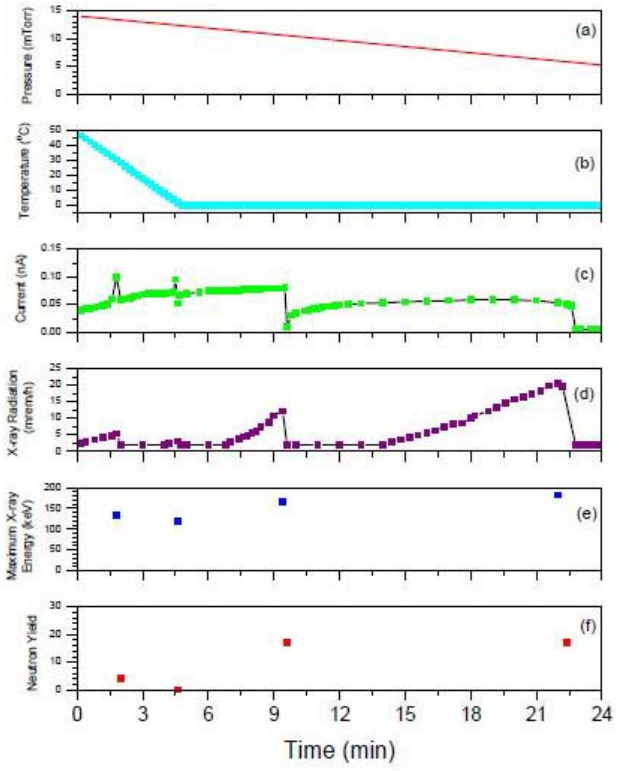

FIGURE 4 SAME AS FIGURE 3 FOR A RUN AT THE LATER STAGE OF OUR MEASUREMENTS

Taking the efficiency (Gonzalez Trotter et al, 2009) and solid angle of our neutron detectors into account, the number of neutrons produced in our work is 3.3 neutrons per second with a 15% uncertainty, which is mostly due to counting statistics and the uncertainty in the neutron detection efficiency (~3%). For comparison, using our present tritiated-target without any dead layer and assuming a D_2^+ energy and current of 170 keV and 1 nA, respectively, one should expect theoretically about 10^6 neutrons per second during a 100 second time interval.

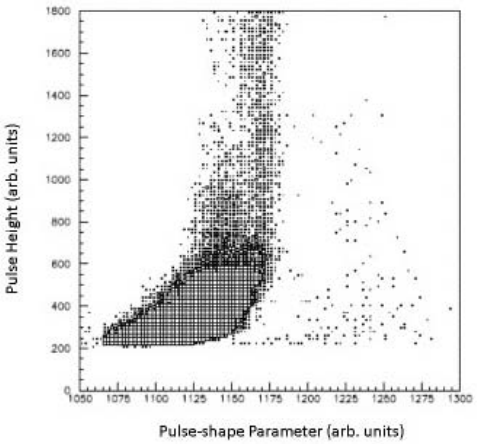

FIGURE 5 TWO-DIMENSIONAL PRESENTATION OF NEUTRON DETECTOR PULSE HEIGHT VERSUS PULSE-SHAPE PARAMETER. THE INTENSE BAND OF EVENTS TO THE LEFT OF CHANNEL 1190 IS DUE TO PILE-UP X-RAY EVENTS AND ENVIRONMENTAL GAMMA-RAY BACKGROUND, WHILE THE EVENTS TO THE RIGHT ARE DUE TO NEUTRONS FROM THE $^3H(d,n)^4He$ REACTION

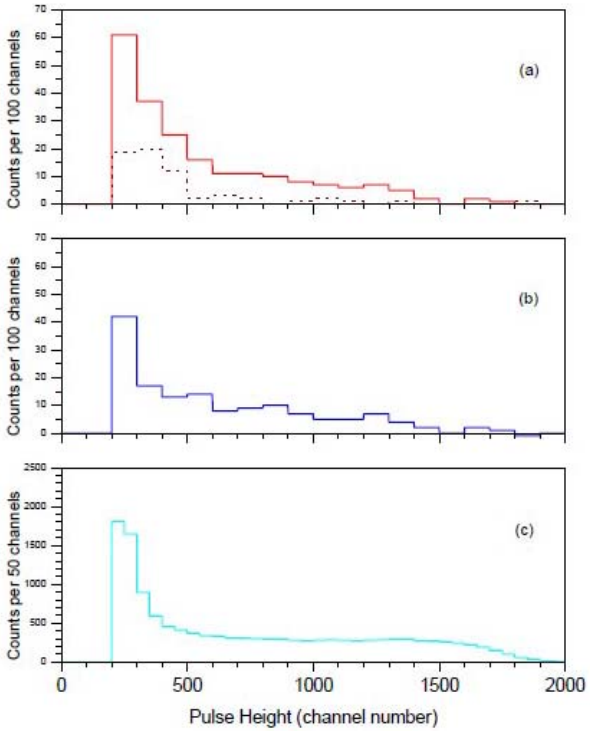

FIGURE 6 NEUTRON ENERGY SPECTRA OBTAINED FROM THE REACTION $^3H(d,n)^4He$ WITH DETECTOR #1: (a) SOLID-LINE HISTOGRAM: 9 COOL-DOWN RUNS OF PYROELECTRIC CRYSTAL ARRANGEMENT LASTING A TOTAL OF 74 .3 MINUTES; DASHED-LINE HISTOGRAM: NATURAL NEUTRON BACKGROUND SPECTRUM MEASURED DURING 74.3 MINUTES WITH PYROELECTRIC CRYSTALS AT ROOM TEMPERATURE, (b) DIFFERENCE SPECTRUM, (c) NEUTRON ENERGY SPECTRUM OBTAINED WITH 14.8 MeV NEUTRONS PRODUCED VIA THE REACTION $^3H(d,n)^4He$ WITH A DEUTERON BEAM ACCELERATED BY THE TUNL TANDEM VAN DE GRAAFF ACCELERATOR USING THE TRITIATED TARGET EMPLOYED IN (a).

Auxilliary Measurements and Results

The published studies involving neutrons from the $^2H(d,n)^3He$ reaction clearly showed that it is important to perform experiments with the deuterium gas

replaced by regular hydrogen gas to really make sure the quoted neutron yield is not just an artifact of misidentified pile-up X-ray events. In our present work with the $^{3}H(d,n)^{4}He$ reaction we did such tests, which resulted in zero neutron yield above background.

Furthermore, it is also very helpful to irradiate the neutron detectors used in the pyroelectric studies with neutron beams produced by conventional particle accelerators using the reaction of interest. To our knowledge, this has not been done by any other group working with pyroelectric crystals. We felt strongly that such tests are necessary, and therefore, reported a spectrum for the $^{2}H(d,n)^{3}He$ reaction in (Tornow et al, 2010). Of course, computer simulations, as done by the UCLA and RPI groups for the $^{2}H(d,n)^{3}He$ reaction (Geuther, Danon, and Saglime, 2006; Naranjo, Gimzewski, and Putterman, 2005) and by the UCLA group for the $^{3}H(d,n)^{4}He$ reaction (Naranjo, Putterman, and Venhaus, 2010), are very helpful, but the real test is an experiment, where adjustable free parameters (for example the light-output function of the neutron detector) are not available.

Safety regulations at TUNL allow operation of tritiated targets only in target rooms at the high-energy end of the tandem accelerator. Therefore, in contrast to our previous work involving the $^{2}H(d,n)^{3}He$ reaction, we could not attach our tritiated target to a beam line coupled directly to one of TUNL's ion sources, which are typically operated at potentials between 50 kV and 80 kV. To circumvent this problem, we directed a 1.8 MeV deuteron beam, the lowest energy deuteron beam available at the high-energy end of the tandem accelerator, onto a target cell containing our tritiated target as beam stop. A schematic of this target cell is shown in Figure 7. A 6.35 μm thick Havar foil separated the accelerator vacuum from the tritiated target foil. This foil slowed down the incident deuterons such that they experience the $^{3}H(d,n)^{4}He$ resonance located at about 106 keV. The volume between the Havar foil and the tritiated target foil was filled with helium at a pressure of 1.5 atm. Neutron detector #1 was placed at a distance of 1 m from the tritiated target at 0° relative to the incident deuteron beam (see Figure 7). Of course, the Havar foil caused a substantial energy straggling of the deuteron beam passing through it. However, the narrow resonance structure of the $^{3}H(d,n)^{4}He$ reaction basically restricted the resulting neutron energy spread to be only ± 50 keV with mean energy of 14.8 MeV. The neutron energy spectrum obtained with neutron detector #1 is shown in Figure 6 (c). Clearly, the spectrum shown here is very similar to the one of Figure 6 (b), confirming that indeed $^{3}H(d,n)^{4}He$ neutrons were produced with the pyroelectric crystal setup.

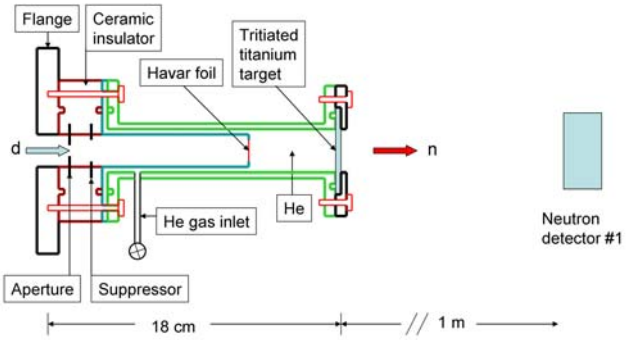

FIGURE 7 TARGET CELL USED TO PRODUCE $^{3}H(d,n)^{4}He$ NEUTRONS WITH TANDEM VAN DE GRAAFF ACCELERATOR, AND LOCATION OF NEUTRON DETECTOR #1. THE DEUTERON BEAM ENTERING ON THE LEFT SIDE IS PRODUCED BY TUNL'S TANDEM VAN DE GRAAFF ACCELERATOR

Future Work

In order to increase the neutron yield, several improvements are necessary.

(a) First, our chamber must be connected directly to a tritium monitor in order to determine whether any tritium is released from the tritiated-titanium target at temperatures of about 150° C. This may allow us to return to our standard operating temperature of 130° C, which was used for the $^{2}H(d,n)^{3}He$ studies (Tornow et al, 2010). As a result, the achievable acceleration potential should increase to above 200 kV. In addition, we would have the opportunity to optimize the cooling rate.

(b) Second, a tritiated-titanium target can easily be mounted on the currently naked face of the two-crystal arrangement. Two targets have been used in (Tornow et al, 2010) for our neutron production studies involving the reaction $^{2}H(d,n)^{3}He$.

(c) Third, to minimize oxidation of the titanium layer of the tritiated target, our vacuum system, and materials used inside of the chamber have to be carefully scrutinized for its potential of oxygen release. In addition, the deuterium gas has to be of higher purity than currently used.

(d) Fourth, other types of tritiated targets should be considered as well. Finding a suitable tritiated target without dead layer will be a very important, if not the most important step, to increase the useful tritiated target thickness, which currently limits the neutron yield. We are trying to acquire

tritiated polyethylene, which could be evaporated onto the exposed $LiTaO_3$ faces.

We expect that improvements in (a), (b), and (c) will increase the neutron yield by one to two orders of magnitude. Any further increase will rest on the availability of tritiated targets without a substantial dead layer. Here, one could expect an additional increase in neutron yield of a few orders of magnitude.

Conclusions

In summary, using a pyroelectric double-crystal arrangement, positively charged deuterium ions have been produced and accelerated towards a tritiated titanium target to produce 14 MeV neutrons via the fusion reaction $^3H(d,n)^4He$. The pyroelectric effect is used to provide the acceleration potential by heating or cooling the crystals. The low power needed for accomplishing the temperature changes can easily be produced by a small solar panel. As a result, solar energy can be reconverted into nuclear fusion energy. If the present approach can be improved and scaled up considerably, far reaching practical applications could be envisioned.

Acknowledgements

We thank Bret Carlin and Alexander Crowell for their contributions to this work, which was supported partially by the US Department of Energy, Office of Nuclear Physics under Grant No. DE-FG02-97ER41033.

References

Geuther, J., Danon, Y., "Nuclear Reactions Induced by a Pyroelectric Accelerator", Physical Review Letters, 96, 054803-1-4, 2006.

Geuther, J.A., Danon, Y., "Enhanced Neutron Production from Pyroelectric Fusion", Journal of Applied Physics, 90, 174103-1-3, 2007.

Gillich, D., Kovanen, A., Herman, B., Fullem, T., Danon, Y., "Pyroelectric Crystal Neutron Production in a Portable Prototype Vacuum System", Nuclear Instruments and Methods in Physics Research A, 602, 306-310, 2009.

Gonzalez Trotter, D.E., Salinas, F., Tornow, W., Crowell, A.S., Howell, C.R., Schmidt, D., Walter, R.L. "Neutron Detection Efficiency Determinations for the TUNL Neutron-Neutron and Neutron-Proton Scattering Length Measurements", Nuclear Instruments and Methods in Physics Research A, 599, 234-242, 2009.

Marion, J.B. and Fowler, J.L., eds. "Fast Neutron Physics", Interscience Publishing Inc., 690-698, 1960.

Naranjo, B., Gimzewski, J.K., Putterman, S. "Observation of Nuclear Fusion Driven by a Pyroelectric Crystal", Nature (London), 434, 1115-1117, 2005.

Naranjo, B., Putterman, S., Venhaus, T. "Pyroelectric Fusion Using a Tritiated Target", Nuclear Instruments and Methods in Physics Research A, 632, 43-46, 2011.

Tang, V. et al. "Neutron Production From Feedback Controlled Thermal Cycling of a Pyroelectric Crystal", Review of Scientific Instruments, 78 (12), 123504-1-4, 2007.

Tornow, W., Corse, W., Crimi, S., Fox, J., "Neutron Production With a Pyroelectric Double-Crystal Assembly Without Nano-tip", Nuclear Intruments and Methods in Physics Research, A624, 699-707, 2010.

Tornow, W., Lynam, S.M., Shafroth, S.M. "Substantial Increase in Acceleration Potential of Pyroelectric Crystals", Journal of Applied Physics, 107, 063302-1-4, 2010.

Tornow, W., Shafroth, S.M., Brownridge, J.D. "Evidence for Neutron Production in Deuterium Gas With a Pyroelectric Crystal Without Tip", Journal Applied Physics, 104, 034905-1-8, 2008.

Tornow, W., Taylor, B.W., Shafroth, S.M. "Energy and Momentum Analysis to Determine the Composition of Ion Beams Produced by Pyroelectric Crystal Accelerators", TUNL Progress Report L, 122-123, 2011.